Research Square

Preprints are preliminary reports that have not undergone peer review.
They should not be considered conclusive, used to inform clinical practice,
or referenced by the media as validated information.

Development of PEBA-PEMA Blend Membranes for the Pervaporation Separation of 1- Butanol from Aqueous Solutions

Praveenkumar Denganavar
Dayananda Sagar University
Santosh K. Choudhari
santoshchoudhari-chem@dsu.edu.in
Dayananda Sagar University
Aditya D. S.
Jain University
S. K. Nataraj
Jain University
Ashok Sajjan
KLE Technological University

Article

Keywords: Biofuel, Pervaporation, Butanol, Blend Membrane, Polyether block amide, Polyethyl methacrylate

Posted Date: May 1st, 2026

DOI: https://doi.org/10.21203/rs.3.rs-9422295/v1

License: This work is licensed under a Creative Commons Attribution 4.0 International License. Read Full License

Additional Declarations: No competing interests reported.

Abstract

The escalating global demand for sustainable energy has intensified the pursuit of advanced biofuels, with biobutanol recognized as a next-generation alternative due to its superior fuel properties. However, commercial-scale biobutanol production remains constrained by issues of product inhibition, low recovery yields, and energy-intensive separation processes. Herein, we report development of high-performance polymeric blend membranes prepared using Hansen's solubility parameters approach for the pervaporation separation of butanol from aqueous solutions. The membranes comprised of polyether block amide (PEBA) and polymethyl methacrylate (PEMA), engineered for efficient butanol recovery through pervaporation. The membrane (PBPM-5) containing 5 wt% of PEMA achieved the best PV separation, yielding a flux of 0.19 $kgm^{-2}h^{-1}$ and a separation factor of 15.5, which is a 50% enhancement in flux and a two-fold raise in the separation factor as compared to the pristine PEBA membrane. Increase in PV operation temperature and feed butanol content showed simultaneous enhancement in both the separation factor and flux for the PBPM-5 membrane. Separation of butanol from multi-component mixture showed decrease in the performance indicating the presence of strong coupling effect. This work shows the PV butanol separation capability of PEBA2533 can be significantly enhanced with the judicial blending of small amount of PEMA polymer.

1. Introduction

Elevated oil prices, heightened demand, diminishing fossil fuel reserves, and environmental issues have sparked a fresh enthusiasm in the manufacturing of fuels from biomass (also known as "biofuels") in recent years [1]. Biobutanol, or n-butanol, has recently garnered significant attention as an advanced biofuel. It possesses multiple advantages compared to methanol and ethanol, including superior energy content, the possibility for a greater blending percentage with petrol, reduced vapor pressure, and diminished hygroscopic properties. It has the potential to be implemented within the existing transportation fuel distribution system [2]. Butanol can be synthesized through the fermentation of carbohydrate substrates obtained from biomass employing *Clostridium acetobutylicium* or *C. beijerinckii* in anaerobic environments, which is commonly referred to as the ABE (Acetone-Ethanol-Butanol) fermentation process [3]. There are still a number of unanswered issues about the technological and financial feasibility of the bioproduction of butanol. Product inhibition by butanol during bioprocessing is a major obstacle in ABE fermentation, leading to reduced productivity, lower butanol yields, and very low concentrations (< 3 wt%), which significantly raise downstream processing costs. Two strategies address this challenge [4]: One involves genetically engineering microorganisms for ABE fermentation to sustain their viability and activity even at elevated product concentrations in the fermentation broth. This has the potential to significantly enhance the yield of the product, boost productivity, and elevate concentration, thereby leading to a reduction in production costs. Nevertheless, this remains an unattainable objective for the future. Another strategy involves creating an effective method for the separation and purification of butanol recovery. Furthermore, the methods of product separation and purification will always provide major difficulties even with the possible implementation of microbe alteration. Typically, ABE fermentation products are separated via distillation. However, the low butanol final concentration and enormous energy expenditure make this approach uneconomical [5]. Liquid-liquid extraction, freeze crystallization [6], gas stripping [7], perstraction [8], membrane distillation [9], adsorption [10], and pervaporation [11] are some of the separation techniques that have been investigated for product recovery in ABE fermentation. Pervaporation is considered to be the most the most promising technique among these. Since this is a membrane-based separation method, it has many benefits, including low carbon emissions, great energy efficiency, and environmental sustainability. Its operational flexibility also makes it possible to recover permeate from binary or multi-component mixtures effectively in a single phase.

The entire feasibility of the PV process is substantially impacted by the membrane and its separation efficiency. In recent decades, a variety of polymeric membranes have been developed and employed for the separation of acetone-butanol-ethanol (ABE) components from aqueous solutions [12]. One of them is polyether block amide (PEBA) 2533, a notable example of commercialized PEBA copolymers [13]. This material exhibits remarkable chemical and mechanical properties, alongside impressive heat stability, and demonstrates effective pervaporation performance with respect to alcohol [14–16], PEBA was shown to have a fairly high affinity for butanol [16], and the membrane fabrication process of PEBA is quite straightforward: dissolution-casting and evaporation without the need of any crosslinking chemical or polymerization. These characteristics are helpful for the industrial usage of PEBA membranes. Furthermore, it is observed that PEBA membrane shows higher butanol permeation flux compared to polydimethyl siloxane (PDMS) membrane, which is considered as a benchmark polymer for PV organic solvent separation [17, 18]. However, based on prior reported findings, PEBA membrane pervaporation performance is still falling short of what is needed for real-world applications. A variety of approaches have been explored to improve the performance of PEBA membranes, such as the incorporation of zeolite [19], carbon-based nanomaterials [20, 21], ionic liquids [22], zeolitic frameworks (ZIF) [10], mesoporous crystalline material (MCM-41) [23], and metal organic frameworks [24].

One of the efficient methods to achieve higher separation performance is the development of polymeric blend membranes [25]. It is a very effective technique that integrates the synergistic features of different polymers into a novel composite material, thereby addressing the shortcomings of the individual polymers to achieve desired performance characteristics. Moreover, polymer blends offer numerous advantages owing to their consistency, brevity, and cost-effectiveness. Hence, in the present study, blend membranes composed of PEMA and PEBA were developed and implemented to separate butanol from binary and multi-component aqueous solutions through pervaporation. In view of this, we selected PEMA to blend with PEBA, using Hansen's solubility parameter approach. The Hansen's solubility parameters offer an effective method for evaluating the affinity between polymeric membrane materials and organic solvents, rendering them a valuable resource for identifying appropriate pervaporation membrane materials. Several earlier investigations demonstrated that HSPs has great ability for choosing materials for pervaporation membranes [26–28]. HSP depends on dispersive force (δ_d), polar interaction (δ_p), and hydrogen bonding (δ_h) factors, which are determined using the group contribution technique [29]. Stronger affinity between polymeric membrane material and a solvent is represented by a lower HSPs value difference between them as previously observed [30]. Table 1 illustrates Hansen's solubility parameters for polymers, butanol, and water, from which the total cohesion (δ_t) and distance parameter (Δ) are computed.

Table 1
Hansen's solubility parameters and calculated distance parameters.

Solvent/ Polymer	δ_d	δ_p	δ_h	$\delta_t = \sqrt{\delta_d^2 + \delta_p^2 + \delta_h^2}$	$\Delta = \sqrt{(\delta_{d1} - \delta_{d2})^2 + (\delta_{p1} - \delta_{p2})^2 + (\delta_{h1} - \delta_{h2})^2}$	**Ref.**
Water	15.5	16	42.3	47.80	$\Delta_{PEBA\text{-}Butanol}$ = 9.34	[31]
Butanol	16	5.7	15.8	23.20	$\Delta_{PEBA\text{-}Water}$ = 36.64	
PEBA	17.6	7.6	6.8	20.34	$\Delta_{PEMA\text{-}Butanol}$ = 9.95	
PEMA	18.64	10.52	7.51	22.68	$\Delta_{PEMA\text{-}Water}$ = 35.46	[32]

It is evident from the table that PEBA and PEMA have a strong affinity for butanol, as their δ_t values are much closer to butanol than water. The computed distance parameter between polymers and butanol is significantly lower than that between polymers and water. As the definition states, a smaller distance parameter (Δ) value indicates stronger interaction between the polymer and the solvent. This signifies that both PEBA and PEMA have strong interactions with butanol; hence, a high performance is expected from the blend membranes.

This is the first publication that uses PEBA-PEMA blends for the pervaporation separation of butanol, as far as the authors are aware. The PV performance of membranes for butanol separation is evaluated in terms of flux and separation factor. The physical and chemical characteristics of the synthesized membranes were investigated. The influence of blend composition, temperature, feed butanol concentration, and multicomponent mixture on separation performance was examined.

2. Experimental

2.1. Materials

PEBAX-2533 polymer was procured from Arkema (France). PEMA was obtained from Sigma-Aldrich, India. Butanol, ethanol, and acetone were procured from S D Fine Chemicals Limited, Mumbai, India. All the chemicals are of analytical grade. Double-distilled water was used throughout the experiment.

2.2. Fabrication of Polymeric Blend Membranes Comprising PEBA and PEMA matrices using Pervaporation technique.

Blended membranes were fabricated via a solution casting approach employing the solution blending method, wherein the requisite proportions of PEBA and PEMA were precisely measured and introduced into 100 mL of *n*-butanol to formulate a 5 wt% (w/v) polymeric solution.

Table 2
Name and composition of the prepared PEBA-PEMA blend membranes.

Blend membrane name	Wt% of PEMA	Wt% of PEBA
PBPM-0 (Pure PEBA)	0	100
PBPM-1	1	99
PBPM-2	2	98
PBPM-5	5	95
PBPM-8	8	92

A series of blend membranes was systematically expressed by varying the PEMA content from 1 to 8 wt% relative to PEBA concentration, as outlined in Table 2. These membranes were designated PBPM-0 to PBPM-8, with each designation reflecting the respective PEMA percentage incorporated into the blend membrane composition. The polymeric constituents were thoroughly solubilized in butanol under continuous magnetic stirring at 80°C for 24 h to ensure complete homogenization. Upon attaining a clear and uniform solution, the mixture was cooled to ambient temperature, following which an appropriate volume of the homogeneous solution was evenly cast into pre-cleaned glass petri dishes. These casting substrates were maintained under quiescent, dust-free atmospheric conditions at room temperature for a period of two days to facilitate solvent evaporation and membrane film formation. The

resultant membranes were subsequently subjected to thermal drying in a hot air oven at 50°C for 24 h to eliminate any residual traces of the organic solvent. For comparative assessment, a control membrane (PBPM-0) composed solely of PEBA was fabricated using the identical methodology, excluding the addition of PEMA as illustrated in Fig. 1. The final membrane thickness was determined using a dial thickness gauge (Model G-2, Misumi, Japan), yielding an average value of approximately 80 ± 5 µm.

2.3. Structural, Morphological, and Surface Characterization of Membranes

The water contact angle of the pervaporation membranes was assessed using a sessile drop contact angle (CA) analyser (Dura-vision Systems India). Attenuated total reflectance infrared spectroscopy (ATR-IR) (Perkin Elmer spectrum GX, Series 59387, UK) was employed to elucidate the functional groups present within the membranes, operating within a range of 4000 to 400 cm^{-1} with a resolution of 2cm^{-1}. Morphological characterization of the membranes was performed using field emission scanning electron microscopy (FESEM) at an accelerating voltage of 15 kV, employing the (FESEM JSM-7100F, USA) instrument. Prior to imaging, all samples intended for SEM analysis were subjected to vacuum drying for a duration of 24 h and subsequently coated with gold via the sputter-coating technique (Hummer 6.2 vacuum sputter). The thermal stability of the membranes was measured using TG-4000-PerkinElmer thermogravimetric analyser (TGA) in N_2 atmosphere. The samples were heated from 30 to 600°C at the rate of 10°C min^{-1}.

2.3.1. Swelling studies

Swelling behavior of the fabricated blend membranes was systematically examined by immersing them in an aqueous solution of butanol (20 g/L) under controlled thermal conditions, employing an electronically regulated oven (Servewell Instruments Pvt. Ltd., India). Prior to the immersion process, the membranes were thoroughly desiccated at 50°C for a duration of 24 h to eliminate residual moisture. After cooling to ambient temperature, the initial dry mass of each membrane specimen was accurately measured. Subsequently, the membranes were submerged in the 2wt% of butanol solution within tightly enclosed sealed glass containers and maintained at 40°C for 24 h to facilitate equilibrium swelling. Post-incubation, the swollen membranes were carefully retrieved and momentarily placed on absorbent blotting paper to remove loosely adhered surface liquid. The samples were gently blotted to remove surface moisture while ensuring their internal structural integrity remained unaltered. The mass of the swollen membranes was immediately recorded using a high-precision digital microbalance (BSA224S-CW, Sartorius, India) with a sensitivity of ± 0.01 mg. Each swelling measurement was conducted in triplicate to ensure statistical reliability, and the mean value was considered for analysis. The percentage degree of swelling (DS) was determined using the following mathematical expression.

$$\textit{Degree of swelling (DS \%)} = \frac{W_s - W_d}{W_d} \times 100 \quad (1)$$

W_s and W_d denote the weights of the swollen membrane and the dried membrane, respectively.

2.4. Pervaporation experiment

PV performance was assessed using a custom-engineered setup. The fabricated membrane was integrated into a stainless-steel PV module with an effective mass transfer area of 19.63 cm^2. Aqueous feed solution was continuously circulated across the membrane surface at a flow rate of 15 L/h, driven by a feed reservoir coupled with a circulation pump. A downstream vacuum pressure of 5 torr was precisely maintained using a high-performance vacuum pump, while the permeate vapor was condensed using cryogenic liquid nitrogen traps and subsequently

collected. To establish steady-state operation, the system was preconditioned for 1 h before initiating the actual PV process, which was conducted over a 2 h duration. The permeation flux was quantified gravimetrically based on the collected condensate mass. Comprehensive compositional analysis of both feed and permeate streams was performed using gas chromatography (GC2024, Shimadzu, Japan) to evaluate separation efficiency as depicted in Fig. 2. The following formulas (2–4) were used to compute the permeation flux (*J*), separation factor (*β*), and pervaporation separation index (PSI) from the experimental data.

$$J = \frac{W}{At} \quad (2)$$

$$\beta = \frac{\raisebox{1ex}{\$}P_o\raisebox{-1ex}{\$}/\raisebox{1ex}{\$}P_w\raisebox{-1ex}{\$}}{\raisebox{1ex}{\$}F_o\raisebox{-1ex}{\$}/\raisebox{1ex}{\$}F_w\raisebox{-1ex}{\$}} \quad (3)$$

$$PSI = J(\beta\text{-}1) \quad (4)$$

Where *W* denotes the weight of permeate (kg), *A* signifies the active membrane area (m^2) in contact with feed, and *t* represents the PV experiment duration (h). P_o, P_w, F_o, and F_w represent the mass fractions of organic compounds and water on the permeate and feed sides, respectively.

3. Results and Discussion

3.1. Characterization of membranes

3.1.1. ATR-IR spectroscopy

The chemical structures and composition of varying PEMA content in different membranes were characterized by ATR-IR analysis as shown in Fig. 3. For the pure PEBA membrane (PBPM-0), distinct features indicative of amide functionalities was observed at 3296 cm^{-1} (N–H stretching), 1740 cm^{-1} (C = O stretching), and 1640 cm^{-1} (N–H bending). The absorption peaks observed at 2926 cm^{-1} and 2847 cm^{-1} corresponds to the asymmetric and symmetric stretching vibrations of methylene ($–CH_2–$) groups, respectively. A prominent peak observed at 1105 cm^{-1} is associated to C–O–C ether linkages. Upon incorporation of PEMA, the blend membranes exhibited additional absorption features distinctive of the polymer backbone. Notable peaks appeared at 1457 cm^{-1} and 1364 cm^{-1}, corresponding to $–CH_2–$ and $–CH_3$ bending vibrations, respectively. The ester functionalities of PEMA were evident from the C–O stretching at 1203 cm^{-1} and an additional ester C = O stretching band near 1640 cm^{-1} is overlapping with the amide signal. Further, a peak at 1097 cm^{-1} was assigned to C–O–C bonds, indicating ether linkages. Lower-wavenumber bands at 983 cm^{-1}, 840 cm^{-1}, and 745 cm^{-1} were ascribed to *trans* CH_2 wagging, C–C stretching, and *cis* CH_2 wagging modes, respectively, confirming the presence of PEMA-specific structural changes [33, 34].

3.1.2. X-ray diffraction

The crystalline structure of pure PEBAX 2533, PEMA and the PEBA-PEMA blend membranes were examined using X-ray diffraction, as shown in Fig. 4. Pure PEBA exhibits a broad peak at 20 degrees, indicating a semi-crystalline nature which corresponds to the crystalline PA segments. Additionally, there are diffraction peaks at 2θ values around 10° to 14° and 23°, although with lower intensity, which are associated with the amorphous PE segments within the PebaX structure which aligns with previously reported results [35, 36]. The XRD spectrum for pure PEMA usually shows two diffraction peaks at about 2θ is 12° and 19°. These peaks are wide and not symmetrical, which suggests that the polymer chains are not perfectly ordered within the crystal lattice and that there are defects in the arrangement.

PEMA is characterized by its amorphous nature, which is further highlighted by the broadness of these Bragg peaks, which corresponds with previously established result [37]. For blend membranes (PBPM-1 to PBPM-8) with increasing PEMA content, the characteristic diffraction peak of PEBA at 10° to 14° gradually diminishes and eventually disappears for PBPM-8, indicating suppression of crystalline ordering and a transition toward a predominantly amorphous morphology. This behavior confirms enhanced polymer chain miscibility and increased structural disorder within the blend system.

3.1.3. Thermal gravimetric analysis

TGA was employed to investigate the thermal stability and decomposition characteristics of the membranes. This analysis was performed under a controlled heating regime to monitor the weight loss as a function of temperature, thereby elucidating the membranes' thermal durability. As illustrated in Fig. 5, the pristine and blended membranes exhibited one stage of thermal degradation, with notable weight loss proceedings observed at approximately 300.12°C, 331.24°C, 363.62°C, 398.45°C, and 439.86°C. These transitions are primarily associated with the breakdown of polymeric chains and the volatilization of low molecular weight fragments [38]. In the case of the PEMA-blended membranes, the thermal degradation profiles shifted depending on the PEMA concentration. The observed variation in decomposition temperatures across the membranes suggests enhanced thermal resistance, which can be attributed to the formation of a more robust hybrid network. The improved thermal stability is likely a result of the synergistic interaction between PEBA and PEMA within the polymer matrix. Specifically, the introduction of PEMA, which in turn restricts polymer chain mobility, elevates the activation energy required for degradation, and delays the onset of thermal decomposition [39].

3.1.4. Contact angle (CA) measurements

The surface wettability of the PEBA–PEMA blend membranes was characterized via static water contact angle measurements using the sessile drop method, the CA was recorded after 10 secs using side-view imaging. As illustrated in Fig. 6, the incorporation of PEMA led to an incremental rise in CA, reflecting decreased surface wettability. The pristine PEBA membrane (PBPM-0) exhibited a contact angle of 47.48° ± 0.4°, which increased progressively with PEMA incorporation to 51.44° ± 0.5° (PBPM-1), 54.07° ± 0.5° (PBPM-2), 55.9° ± 0.5° (PBPM-5), and peaking at 61.85° ± 0.4° for (PBPM-8). Digital images of contact angle measurements are presented in Fig. 6. This rising trend in contact angle is attributed to the increasing content of PEMA, which possesses a less polar backbone relative to the polar functionalities present in PEBA. The PEBA matrix, rich in amide and ether segments, inherently exhibits greater surface polarity, facilitating strong hydrogen bonding with water molecules[40]. In contrast, the introduction of PEMA leads to the suppression of surface polarity and disruption of hydrogen-bonding interactions, thereby reducing the surface energy and enhancing hydrophobic characteristics [41].

3.1.5. Scanning electron microscope

The surface morphology of the fabricated membranes was characterized using FESEM, as depicted in Fig. 7. The micrographs provide insight into the morphological evolution of the membrane surface as a function of increasing PEMA content, ranging from 0 to 10 wt%. For the pure PEBA membrane (PBPM-0) as represented in Fig. 7(a1-a3), a relatively uniform surface morphology is observed, indicating a hybrid homogenous surface. As PEMA was incorporated into the PEBA matrix (PBPM-1 to PBPM-8 membranes), a distinct evolution in surface morphology was observed. With increasing PEMA concentration, the membrane surface exhibited progressive modifications associated with altered microstructural rearrangement. In particular, PBPM-1 and PBPM-2 membranes retained a

relatively compact surface architecture; however, subtle textural variations indicated the initial stages of microphase separation, attributed to partial miscibility between the polymer components [42].

At PBPM-5 membrane in Fig. 7(d1-d3), the micrographs reveal the emergence of distinct granules or micro-aggregates embedded on the membrane surface, attributed to the decreased compatibility between the PEBA matrix and the PEMA. This is indicative of phase segregation and the disruption of the polymeric chain packing, resulting in heterogeneous surface features. The PBPM-8 membrane exhibits surface coarseness with increased granularity and reduced smoothness. Such morphological irregularities are symptomatic of significant immiscibility and domain separation within the polymer blend. Despite these changes, all membranes across the composition range remain free from cracks or interfacial voids, suggesting that the interfacial adhesion and mechanical integrity of the membranes are preserved[43].

The observed morphological transformation aligns with the known structure of PEBA, a block copolymer comprising 80% flexible polyether (PE) segments and 20% rigid polyamide (PA) segments. The introduction of PEMA perturbs the ordered microphase-separated domains of PEBA, promoting morphological heterogeneity[35]. At higher PEMA loadings, extensive disruption leads to agglomeration and surface roughening, which may affect the membrane's performance characteristics [44]. The FESEM analysis confirms that the miscibility and structural compatibility of PEMA within the PEBA matrix deteriorate beyond 5 wt%, manifesting in increased surface roughness and granular features. The absence of defects such as cracks or voids validates the structural soundness of all prepared membranes.

3.2. Effect of PEMA blending on pervaporation performance

Figure 8(a) illustrates the impact of PEMA loading weight percentages influence on the pervaporation performance of PEBA-PEMA blend membranes for the separation of an aqueous butanol solution containing 20 g/L butanol at 40°C. Pure PEBA membrane (PBPM-0) showed a flux value of 0.12 $kgm^{-2}h^{-1}$ and separation factor around 8, which are in good accordance with previously reported values [10, 16, 45].

The results indicate that blending of PEMA led to a simultaneous enhancement in both flux and separation factor up to an optimal loading of 5 wt%, beyond which a decline in performance was observed at 8 wt%. The increase in flux and separation factor values with the addition of PEMA is due to an increase in membrane hydrophobicity and membrane swelling. The membrane hydrophobicity was analysed through measuring contact angle, and swelling studies were conducted to measure swelling percentage; the attained values are presented in Fig. 8 (b). Pristine PEBA indicated a water contact angle of 48°, which steadily increased with the addition of PEMA, and the membrane showed a contact angle of 62° for 8% of PEMA. Similarly, the inclusion of PEMA also caused an increase in membrane swelling, which went from 2.1% for pure PEBA to 4% for 8 wt% PEMA blending.

This clearly demonstrates that the addition of PEMA causes an increase in membrane hydrophobicity and swelling, which in turn causes a higher absorption and permeation of butanol, leading to an increase in separation factor and flux. However, membrane blend compatibility decreased at greater percentages of PEMA, which has decreased flux and separation factor as evident from SEM analysis. The membrane PBPM-5, which contained 5 wt% PEMA, exhibited the maximum flux of 0.19 $kgm^{-2}h^{-1}$, about 50% higher than the flux value of the PBPM-0, and a separation factor of 16, which is approximately two-fold higher than that of the pristine PEBA membrane. In general, there exists a trade-off relationship between flux and separation factor [22], and very few modified membranes have seldom overcome this problem. In the past, few researchers were able to solve this trade-off relationship by developing mixed matrix membranes [20, 46]. Interestingly, in the current scenario as well, the developed blend membranes are

capable of surmounting this obstacle. This phenomenon may be attributed to the increased hydrophobicity and adequate swelling of membranes.

The pervaporation separation index is an important metric. It is a relative evaluation of a membrane's separation ability and determined as the product of flux and separation factor [47]. This index serves as a useful parameter to select the membrane with the ideal balance of permeation flux and separation factor. The PSI values were determined according to Eq. 4, and the results are shown in Fig. 9. It has been observed that the PSI values increased as the PEMA content in the membrane gradually increased up to 5 wt% and then declined for 8 wt%. Increasing PSI values are attributed to simultaneous increase in both flux and separation factor values. The membrane containing 5 wt% PEMA had the maximum PSI value of 2.7, while the membrane with 8 wt% PEMA had the lowest PSI value of 0.76. This reduction in PSI is due to both reduced flux and separation factor values resulting from blend incompatibility. Thus, the PBPM-5 membrane with 5 wt% of PEMA was chosen for further investigations.

3.3. Effect of temperature on PV butanol separation

To study the influence of feed temperature on pervaporation, PBPM-5 membrane was employed to separate 20 g/L butanol aqueous solution at various temperatures ranging from 30 to 60°C. Figure 10(a) shows the observed total flux and separation factor values. Both the total flux and separation factor increased as the feed temperature increased. To more clearly analyse the results, individual fluxes (water and butanol flux) values were evaluated and presented as a function of temperature, as seen in Fig. 10(b). It is evident from the figure, increased water and butanol fluxes account for the overall flux increase. The increase in permeation flux primarily results from an enhanced transmembrane driving force and an increase in the free volume of the membrane. As temperatures rise, the vapour pressure on the feed side increases, while the vapour pressure on the permeate side remains constant. Consequently, the driving force across the membrane increases, resulting in higher mass transport. PEBA-2533 is a thermoplastic elastomer composed of a multiblock copolymer with 20% polyamide (PA) hard segments and 80% flexible polyether (PE) soft segments. The glass transition temperature of the hard segment is around 108°C, while that of the soft segment is -78°C, which is significantly low[48]. The rigid segment polyamide (PA) provides the mechanical strength; on the other hand, the polyether (PE) soft segment is responsible for continuous pathways for diffusion of molecules. At higher temperatures, the frequency and amplitude of polymer chain jumping in the PE soft segment region increases there by increasing the free volume in the membrane. This results in a greater permeation of molecules through the membrane. The increased separation factor at higher temperatures is attributed to an increase in butanol permeation, which is more likely due to higher butanol solubility in the membrane at higher temperatures.

The temperature dependency of permeate flux follows an Arrhenius equation, as illustrated in Fig. 11, which is common in pervaporation [49]. A positive activation energy indicates that flux rises with elevated temperature, a phenomenon commonly reported in many PV technique[50]. If the perceived activation energy E_a for the component permeating through the membrane is higher, it means that the behavior is more sensitive to changes in temperature [51]. As seen in Fig. 11, butanol appears to have a larger activation energy than water; this shows that butanol permeation is more sensitive towards temperature; as a result, higher temperatures may yield greater selectivity.

3.4. Effect of feed butanol concentration on PV performance

The effect of butanol feed concentration on PV separation was studied by employing membrane PBPM-5. The operating temperature was kept at 60°C, and the feed butanol concentration was varied from 1 to 20 g/L. Figure 12(a) displays the observed flux and separation factor values. As the feed butanol concentration increases from 1 g/L to 20 g/L, both total flux and separation factor simultaneously increase. The total flux value increased

from 0.20 to 0.28 $kgm^{-2}h^{-1}$, while the separation factor increased from almost 1.8 to 19.3. To explain these results, individual fluxes (butanol and water) were calculated and plotted against the butanol feed concentration, as seen in Fig. 12(b).

According to Fig. 12(b), the water flux remained relatively stable, on the other hand, butanol flux gradually increased from 7×10^{-3} to 70×10^{-3} $kgm^{-2}h^{-1}$. Several other researchers also reported this relative constancy of water flux [52, 53]. Additionally, the change in the water concentration as the primary component of the feed solution is not as significant as that of organic compounds. In contrast, the activity and partial vapour pressure of butanol increase progressively as the concentration of feed butanol increases, ensuing in a larger butanol flux. Thus, the enhancement in flux and separation factor is mainly attributed to the increased butanol permeation at higher feed butanol concentrations.

Interestingly, in several cases, higher feed organic concentrations result in increased flux accompanied by lower separation efficiency due to plasticization and swelling effect [54, 55]. But in the present study, although the membrane gave a higher flux, the separation factor did not go down. This indicates that the plasticization effect is absent and the membrane has adequate swelling in the studied feed butanol concentration.

3.5. Pervaporation performance for model ABE solution

Butanol is the main product and also the principal inhibitor in ABE fermentation; so, its recovery from fermentation is quite important. Considering that acetone and ethanol are also produced as by-products, it is necessary to investigate the impact of these chemicals on PV separation of butanol in ABE solution. Therefore, PBPM-5 membrane was employed to separate butanol from model ABE solution at 60°C. To simulate actual fermentation broth concentrations, ABE model solution was prepared by dissolving 6 g/L of acetone, 12 g/L of butanol, and 2 g/L of ethanol in a 3:6:1 ratio. Table 3 shows the obtained flux and separation values.

Table 3
Flux and separation factor values for binary and ABE mixture.

Solvent	**ABE mixture**			**Butanol-water binary mixtures**
	Acetone	**Butanol**	**Ethanol**	**Butanol**
Flux ($kgm^{-2}h^{-1}$)	0.05	0.14	0.005	0.25
Separation factor (α)	5.6	9.1	2.7	12

Pervaporation performance followed the order of n-butanol ▯acetone▯ ▯ethanol. This is similar to the previous results obtained by other researchers [16, 46, 56]. F. Liu *et al.*[57] observed that permeation order followed the same order as that of solvent uptake order; hence, they owed this to preferential sorption. These results indicate that sorption is playing a dominant role in the present case. Moreover, the feed chemicals concentration is in order of *n*-butanol (12 g/L) ▯acetone (6g/L) ▯ethanol (2 g/L) and accordingly driving force generated due to partial vapor pressures will be of the order of *n*-butanol ▯acetone▯ ▯ethanol. Therefore, this indicates that preferential sorption and the difference in driving force generated are responsible for the obtained pervaporation results in the present studies.

Upon comparing the butanol permeation results of the ABE mixture with those of a binary butanol aqueous mixture at a similar butanol content, it is evident that both the flux and separation factor are substantially decreased. Butanol flux decreased by almost 44% while separation reduced from 12 to 9.1. This indicates that the presence of other components affected the pervaporative separation of butanol. Acetone, butanol, and ethanol have similar physicochemical features; hence, they interact and couple strongly, reducing butanol permeation during ABE

pervaporation. Similar observations were made by many other previous researchers [54, 56]. Therefore, the coupling effect is a crucial consideration when dealing with multiple component feed mixtures.

4. Conclusion

Usimg Hansen's solubility parameter approach, PEMA was selected to blend with PEBA polymer, and the resultant PEBA-PEMA blend membranes were employed for the pervaporation separation of *n*-butanol from binary aqueous as well as multi-component ABE solutions. Blending of PEMA with PEBA enhanced surface hydrophobicity and increased surface roughness, as indicated by contact angle measurements and SEM images. Application of blend membranes for the PV separation of *n*-butanol from a 20 g/L aqueous solution at 50°C has shown an improvement in both permeation flux and separation factor. Nonetheless, the deterioration of PV performance at higher blend compositions (≥ 8 wt%) due to phase separation imposing limitations on the blending ratio. Membrane PBPM-5, comprising 5 wt% of PEMA, exhibited the highest flux of 0.19 $kgm^{-2}h^{-1}$ and a separation factor of 15.5 which is 50% enhancement in flux and two fold increase in separation factor as compared to the pure PEBA membrane. Increasing the feed operating temperature from 30 to 60°C enhanced both total flux and separation factor due to increased driving force, free volume in the membrane, and higher butanol solubility in the membrane at higher temperatures. At 60°C, the membrane PBPM-5 had the highest flux (0.28 $kgm^{-2}h^{-1}$) and separation factor (18.3). The computed activation energy values indicated that butanol flux is more temperature sensitive than water. The variation in feed butanol content from 1 g/L to 20 g/L resulted an increase in both flux and separation factor, which is attributed to the increase in butanol flux due to higher activity and partial vapour pressure of butanol. PV separation of butanol from the ABE mixture revealed a considerable decrease in flux and separation factor when compared to the binary aqueous solution, indicating the presence of a strong coupling effect.

Over all, the investigation showed that the PV butanol separation capability of PEBA polymer can be considerably improved by the simple process of blending a small quantity of PEMA with PEBA.

Declarations

Declaration of competing interest

The authors declare that they have no known competing financial interests or personal relationships that could have appeared to influence the work reported in this paper.

Funding

This research was funded by Department of Science and Technology, Science and Engineering Research Board (DST-SERB) in New Delhi, India through the Core Research Grant (CRG) (sanctioned no. CRG/2018/003474).

Author Contribution

Praveenkumar Denganavar: Investigation, Formal analysis, Validation, Data curation, Writing – original draft, Santosh K. Choudhari: Visualization, Conceptualization, Methodology, Supervision, Writing – review and editing, Funding acquisition, Project administration, Aditya D S: Formal analysis, S. K. Nataraj: Funding acquisition, Writing – review and editing, Ashok Sajjan: Writing – review and editing.

Acknowledgement

The authors express their sincere gratitude to the Department of Science and Technology, Science and Engineering Research Board (DST-SERB) in New Delhi, India, for funding this research work through the Core Research Grant (CRG) (sanctioned no. CRG/2018/003474).

Data Availability

Data will be made available on request.

References

1. Dellomonaco, C., Fava, F. & Gonzalez, R. The path to next generation biofuels: successes and challenges in the era of synthetic biology. *Microb. Cell. Fact.* **9**, 3 (2010).
2. Çalhan, A. et al. Silica Filled Polyphenylsulfone/Polydimethylsiloxane Composite Membranes for Pervaporation Separation of Biobutanol from ABE Mixtures. *Chem. Eng. Process. - Process. Intensif.* **156**, 108099 (2020).
3. Liu, L. et al. Process optimization of acetone-butanol-ethanol fermentation integrated with pervaporation for enhanced butanol production. *Biochem. Eng. J.* **173**, 108070 (2021).
4. Qureshi, N. *Butanol Recovery from Model Solution/Fermentation Broth by Pervaporation: Evaluation of Membrane Performance*. 17, 175–184 (2018).
5. Oudshoorn, A., Van Der Wielen, L. A. & Straathof, A. J. Assessment of options for selective 1-butanol recovery from aqueous solution. *Ind. Eng. Chem. Res.* **48**, 7325–7336 (2009).
6. Eckert, G. & Schügerl, K. Continuous acetone-butanol production with direct product removal. *Appl. Microbiol. Biotechnol.* **27**, 221–228 (1987).
7. Rochón, E. et al. Bioprocess intensification for isopropanol, butanol and ethanol (IBE) production by fermentation from sugarcane and sweet sorghum juices through a gas stripping-pervaporation recovery process. *Fuel* **281**, 118593 (2020).
8. Merlet, G. et al. In-situ recovery of butanol from ABE fermentation solution by hydrophobic ionic liquid perstraction in tubular membranes assisted with vacuum. *Separation and Purification Technology* 314, 123630 (2023).
9. Liu, G. et al. Selection of eco-efficient downstream distillation sequences for acetone-butanol-ethanol (ABE) purification from *in situ* product recovery system. *Renew. Energy*. **185**, 17–31 (2022).
10. Li, W. et al. Recovery of bio-butanol from aqueous solution with ZIF-8 modified graphene oxide composite membrane. *J. Membr. Sci.* **598**, 117671 (2020).
11. Cheng, C., Yang, D., Bao, M. & Xue, C. Spray-coated PDMS/PVDF composite membrane for enhanced butanol recovery by pervaporation. *J. Appl. Polym. Sci.* **138**, 49738 (2021).
12. Komal, A. et al. Enhancing butanol separation efficiency in pervaporation with ZIF-8 porous liquid infused mixed matrix membranes. *Chem. Eng. Res. Des.* **206**, 43–53 (2024).
13. Liu, K., Tong, Z., Liu, L. & Feng, X. Separation of organic compounds from water by pervaporation in the production of n-butyl acetate via esterification by reactive distillation. *J. Membr. Sci.* **256**, 193–201 (2005).
14. Fouad, E. A. & Feng, X. Use of pervaporation to separate butanol from dilute aqueous solutions: Effects of operating conditions and concentration polarization. *J. Membr. Sci.* **323**, 428–435 (2008).

15. Gu, J. et al. Silicalite-Filled PEBA Membranes for Recovering Ethanol from Aqueous Solution by Pervaporation. *Chem. Eng. Technol.* **32**, 155–160 (2009).
16. Liu, F., Liu, L. & Feng, X. Separation of Acetone-Butanol-Ethanol (ABE) From Dilute Aqueous Solutions by Pervaporation. *Sep. Purif. Technol.* **42**, 273–282 (2005).
17. Böddeker, K. W., Bengtson, G. & Pingel, H. Pervaporation of isomeric butanols. *J. Membr. Sci.* **54**, 1–12 (1990).
18. Yen, H. W., Lin, S. F. & Yang, I. K. Use of poly(ether-block-amide) in pervaporation coupling with a fermentor to enhance butanol production in the cultivation of Clostridium acetobutylicum. *J. Biosci. Bioeng.* **113**, 372–377 (2012).
19. Tan, H., Wu, Y. & Li, T. Pervaporation of *n*- butanol aqueous solution through ZSM-5-PEBA composite membranes. *J. Appl. Polym. Sci.* **129**, 105–112 (2013).
20. Tang, W. et al. Ionic liquid modified graphene oxide-PEBA mixed matrix membrane for pervaporation of butanol aqueous solutions. *J. Membr. Sci.* **581**, 93–104 (2019).
21. Yen, H. W., Chen, Z. H. & Yang, I. K. Use of the composite membrane of poly(ether-block-amide) and carbon nanotubes (CNTs) in a pervaporation system incorporated with fermentation for butanol production by Clostridium acetobutylicum. *Bioresour. Technol.* **109**, 105–109 (2012).
22. Arregoitia-Sarabia, C., González-Revuelta, D., Fallanza, M., Gorri, D. & Ortiz, I. Polymer inclusion membranes containing ionic liquids for the recovery of n-butanol from ABE solutions by pervaporation. *Sep. Purif. Technol.* **248**, 117101 (2020).
23. Tan, H., Wu, Y., Zhou, Y., Liu, Z. & Li, T. Pervaporative recovery of n-butanol from aqueous solutions with MCM-41 filled PEBA mixed matrix membrane. *J. Membr. Sci.* **453**, 302–311 (2014).
24. Liu, S., Liu, G., Shen, J. & Jin, W. Fabrication of MOFs/PEBA mixed matrix membranes and their application in bio-butanol production. *Sep. Purif. Technol.* **133**, 40–47 (2014).
25. Yong, W. F. & Zhang, H. Recent advances in polymer blend membranes for gas separation and pervaporation. *Prog. Mater. Sci.* **116**, 100713 (2021).
26. Mandal, S. & Pangarkar, V. G. Effect of membrane morphology in pervaporative separation of isopropyl alcohol–aromatic mixtures— a thermodynamic approach to membrane selection. *J. Appl. Polym. Sci.* **90**, 3912–3921 (2003).
27. Pal, S. M. & Pangarkar, V. G. Acrylonitrile-based copolymer membranes for the separation of methanol from a methanol–toluene mixture through pervaporation. *J. Appl. Polym. Sci.* **96**, 243–252 (2005).
28. Wang, Y. C. et al. Pervaporation of benzene/cyclohexane mixtures through aromatic polyamide membranes. *J. Membr. Sci.* **185**, 193–200 (2001).
29. Grulke, E. A. Solubility Parameter Values. in The Wiley Database of Polymer Properties (eds Brandrup, J., Immergut, E. H. & Grulke, E. A.) (Wiley, doi:10.1002/0471532053.bra062. (1999).
30. Smitha, B., Suhanya, D., Sridhar, S. & Ramakrishna, M. Separation of organic–organic mixtures by pervaporation—a review. *J. Membr. Sci.* **241**, 1–21 (2004).
31. Knozowska, K. et al. Performance of commercial composite hydrophobic membranes applied for pervaporative reclamation of acetone, butanol, and ethanol from aqueous solutions: Binary mixtures. *Sep. Purif. Technol.* **188**, 512–522 (2017).
32. Grulke, E. A., Bandrup., J., Mmergut, E. H. I. & Grulke, E. A. (eds) *Polymer Handbook* 4th edn, Vol. 2, p. VII698 (Wiley, 1998).
33. Ortega, A., Meléndez-Ortiz, H. I. & García-Uriostegui, L. Ávila-Soria, G. Drug delivery system based on poly(ether-block-amide) and acrylic acid for controlled release of vancomycin. *J. Appl. Polym. Sci.* **135**, 45745 (2018).

34. Ban, Y., Jin, L., Li, Y., Yang, H. & Hu, H. Pyrolysis behaviors of model compounds with representative oxygen-containing functional groups in carbonaceous feedstock over calcium. *Fuel* **335**, 127137 (2023).
35. Sanaeepur, H. et al. Aminosilane cross-linked poly ether-block-amide PEBAX 2533: Characterization and CO2 separation properties. *Korean J. Chem. Eng.* **36**, 1339–1349 (2019).
36. Tan, H., Wu, Y. & Li, T. Pervaporation of *n*- butanol aqueous solution through ZSM-5-PEBA composite membranes. *J. Appl. Polym. Sci.* **129**, 105–112 (2013).
37. Al-Harbi, N. Enhancement of the optical and electrical properties of poly ethyl methacrylate/polyvinyl chloride-zinc sulphide (PEMA/PVC@ZnS) ternary nanocomposite films. *Heliyon* **9**, e21372 (2023).
38. Allayarov, S. R. et al. Influence of γ-radiation on thermal destruction of a cross-linked acrylic polymer. *Polym. Degrad. Stab.* **191**, 109697 (2021).
39. Sharma, S., Acharya, A. D., Thakur, Y. S. & Bisoyi, S. Optimizing BiOCl concentration for enhanced LDPE performance: Investigation of structure, thermal stability, and optical characteristics. *J. Mol. Struct.* **1294**, 136382 (2023).
40. Du, Z., Gong, S., Yu, Z., Pan, K. & Zhang, R. High-Stability hydrophilic PEBA-based composite membrane for efficient pervaporation desalination. *Sep. Purif. Technol.* **360**, 130893 (2025).
41. Ayana, K. D., Ha, C. S. & Ali, A. Y. Comprehensive overview of wood polymer composite: Formulation and technology, properties, interphase modification, and characterization. *Sustainable Mater. Technol.* **40**, e00983 (2024).
42. Vittoria, A. et al. Synthesis of Statistical Multiblock Copolymers through Chain Shuttling Copolymerization with a Thermomechanical Switch Behavior. *Macromolecules* **57**, 1532–1545 (2024).
43. Azarmgin, S. et al. Polyurethanes and Their Biomedical Applications. *ACS Biomater. Sci. Eng.* **10**, 6828–6859 (2024).
44. Soloukipour, S., Saljoughi, E. & Mousavi, S. M. Pourafshari Chenar, M. PEBA/PVDF blend pervaporation membranes: preparation and performance. *Polym. Adv. Technol.* **28**, 113–123 (2017).
45. Wu, G., Li, Y., Geng, Y. & Jia, Z. In situ preparation of COF-LZU1 in poly(ether-*block*-amide) membranes for efficient pervaporation of n-butanol/water mixture. *J. Membr. Sci.* **581**, 1–8 (2019).
46. Liu, S., Liu, G., Zhao, X. & Jin, W. Hydrophobic-ZIF-71 filled PEBA mixed matrix membranes for recovery of biobutanol via pervaporation. *J. Membr. Sci.* **446**, 181–188 (2013).
47. Cerrone, F. et al. Medium chain length polyhydroxyalkanoate (mcl-PHA) production from volatile fatty acids derived from the anaerobic digestion of grass. *Appl. Microbiol. Biotechnol.* **98**, 611–620 (2014).
48. Choi, M. C., Jung, J. Y., Yeom, H. S. & Chang, Y. W. Mechanical, thermal, barrier, and rheological properties of poly(ether-block-amide) elastomer/organoclay nanocomposite prepared by melt blending. *Polym. Eng. Sci.* **53**, 982–991 (2013).
49. Chovau, S., Gaykawad, S., Straathof, A. J. J. & Van der Bruggen, B. Influence of fermentation by-products on the purification of ethanol from water using pervaporation. *Bioresour. Technol.* **102**, 1669–1674 (2011).
50. Aouinti, L. & Belbachir, M. A maghnite-clay-H/ polymer membrane for separation of ethanol–water azeotrope. *Appl. Clay Sci.* **39**, 78–85 (2008).
51. García, V., Pongrácz, E., Muurinen, E. & Keiski, R. L. Pervaporation of dichloromethane from multicomponent aqueous systems containing *n*-butanol and sodium chloride. *J. Membr. Sci.* **326**, 92–102 (2009).
52. Beltran, A. B., Nisola, G. M., Vivas, E. L., Cho, W. & Chung, W. J. Poly(octylmethylsiloxane)/oleyl alcohol supported liquid membrane for the pervaporative recovery of 1-butanol from aqueous and ABE model solutions. *J. Ind. Eng. Chem.* **19**, 182–189 (2013).

53. Zhou, H., Su, Y., Chen, X., Yi, S. & Wan, Y. Modification of silicalite-1 by vinyltrimethoxysilane (VTMS) and preparation of silicalite-1 filled polydimethylsiloxane (PDMS) hybrid pervaporation membranes. *Sep. Purif. Technol.* **75**, 286–294 (2010).
54. Li, Y. et al. PEBA/ceramic hollow fiber composite membrane for high-efficiency recovery of bio-butanol via pervaporation. *J. Membr. Sci.* **510**, 338–347 (2016).
55. Wang, H. et al. Mass transport and pervaporation recovery of aniline with high-purity from dilute aqueous solution by PEBA/PVDF composite membranes. *Sep. Purif. Technol.* **268**, 118708 (2021).
56. Kujawski, J., Rozicka, A., Bryjak, M. & Kujawski, W. Pervaporative removal of acetone, butanol and ethanol from binary and multicomponent aqueous mixtures. *Sep. Purif. Technol.* **132**, 422–429 (2014).
57. Liu, F., Liu, L. & Feng, X. Separation of acetone–butanol–ethanol (ABE) from dilute aqueous solutions by pervaporation. *Sep. Purif. Technol.* **42**, 273–282 (2005).
58. CRediT authorship contribution statement.
59. Praveenkumar Denganavar, S. K. & Nataraj Funding acquisition, Writing – review and editing, Ashok Sajjan: Writing – review and editing, Santosh K. Choudhari: Visualization, Conceptualization, Methodology, Supervision, Writing – review and editing, Funding acquisition, Project administration.

Figures

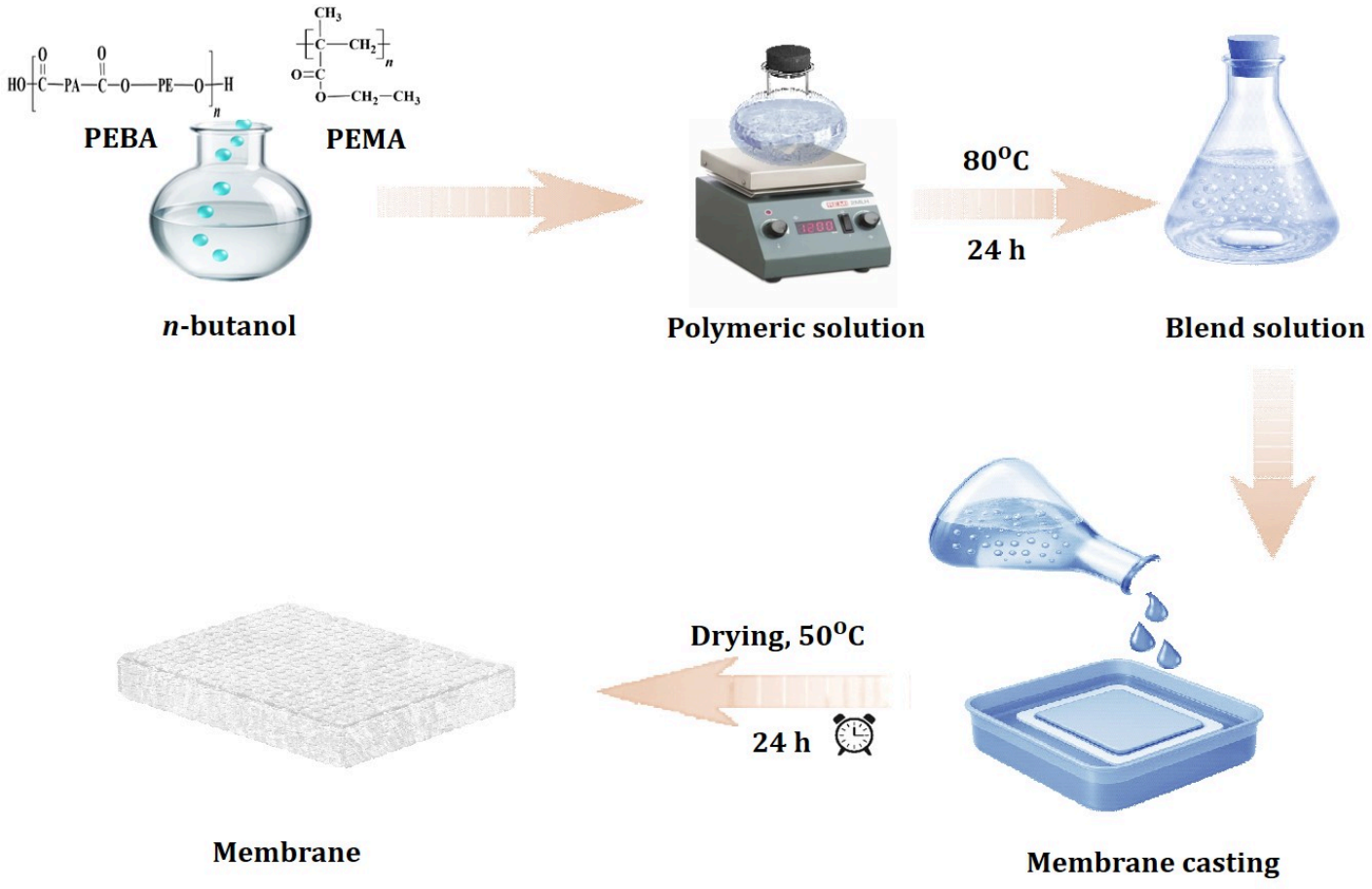


Figure 1

Schematic representation illustrating the fabrication process of PEMA–PEBA blended membranes via solution casting.

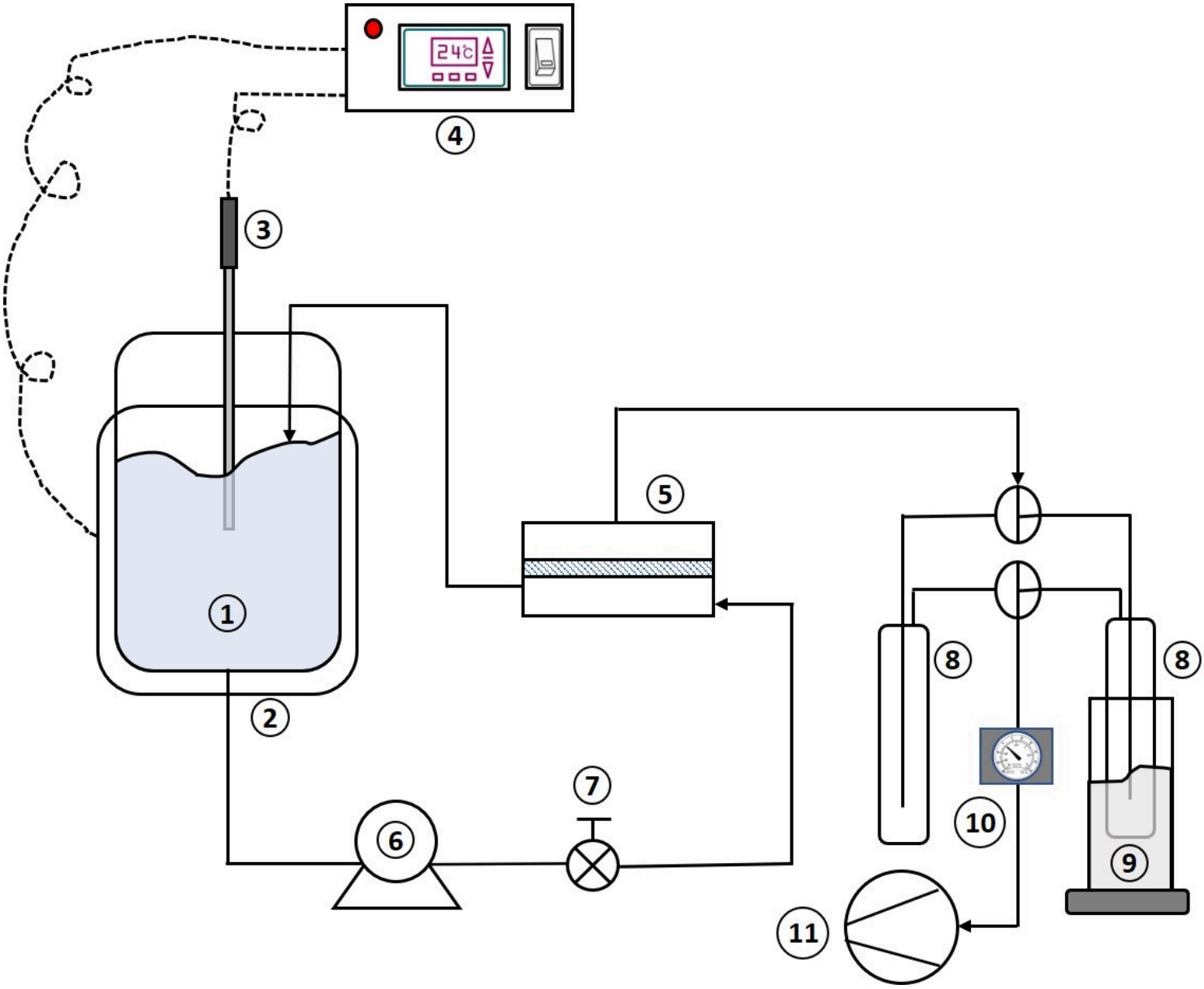


Figure 2

Schematic diagram lab-scale pervaporation setup (1) Feed tank; (2) Heating jacket; (3) Temperature probe; (4) Temperature controller; (5) Membrane permeation cell; (6) Feed circulation pump; (7) Metering valve; (8) Permeate cold traps; (9) Liquid nitrogen container; (10) Vacuum gauze; (11) Vacuum pump.

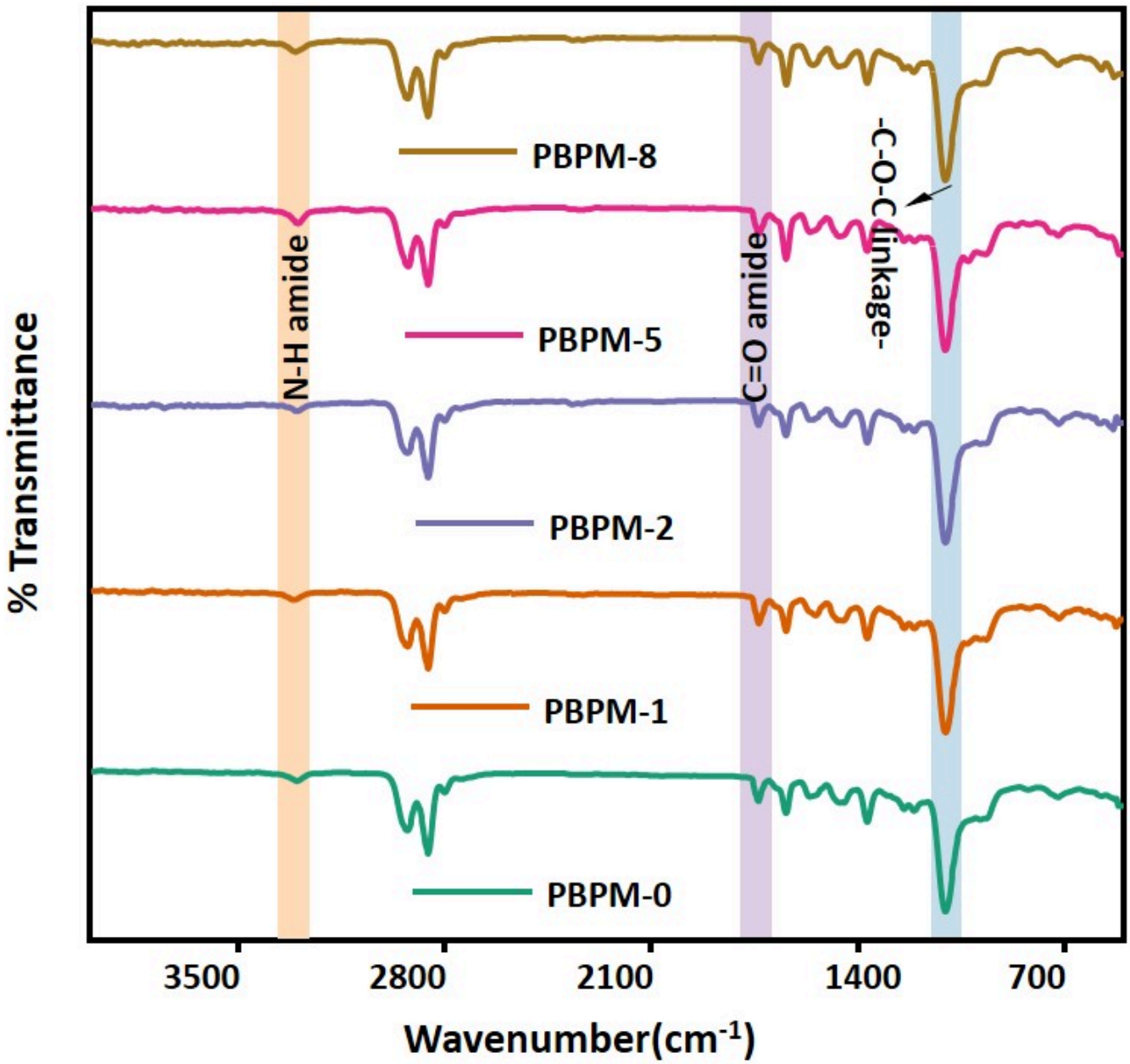


Figure 3

ATR-IR spectra of PBPM-0, PBPM-1, PBPM-2, PBPM-5, and PBPM-8 blend membranes.

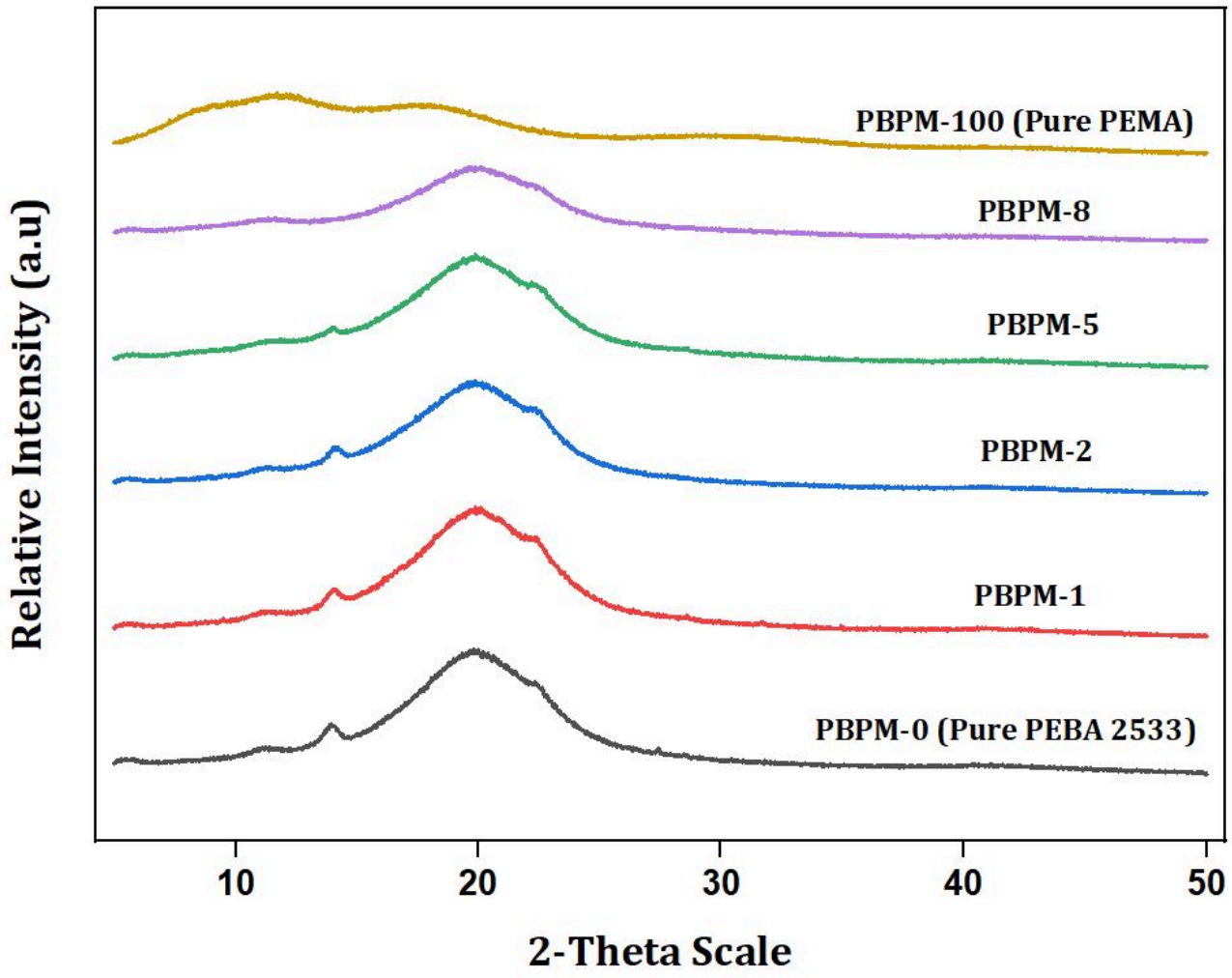


Figure 4

XRD Peaks of PBPM-0, PBPM-1, PBPM-2, PBPM-5, and PBPM-8 blend membranes.

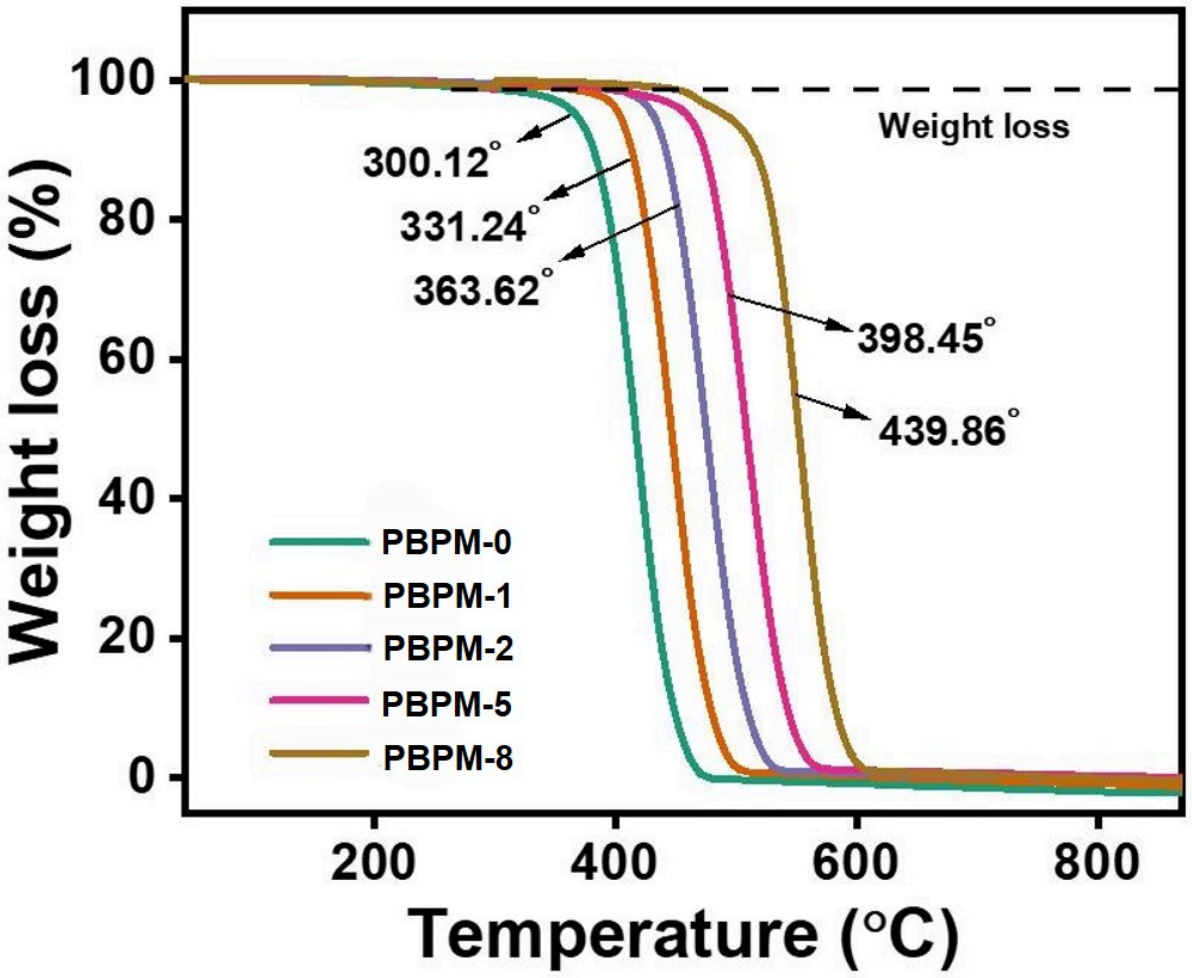


Figure 5

TGA profiles of PBPM-0, PBPM-1, PBPM-2, PBPM-5, and PBPM-8 blend membranes.

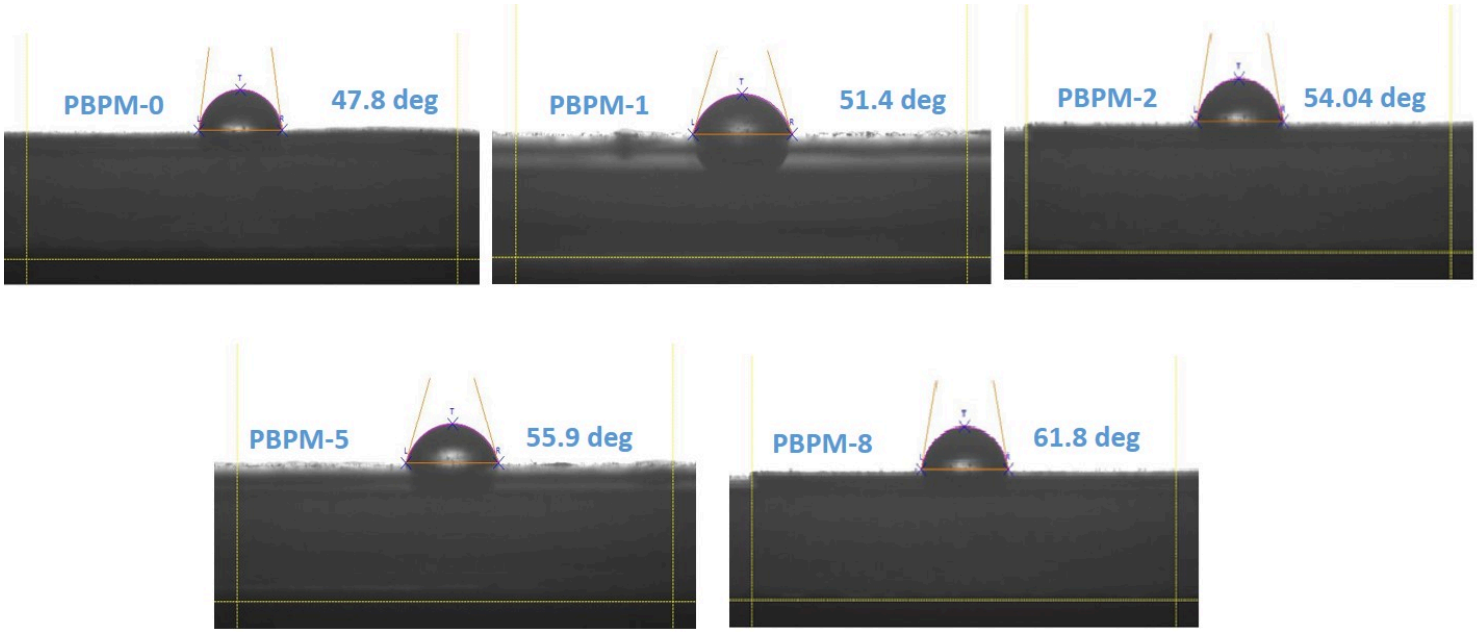


Figure 6

Contact angle images of the pure PEBA and blended membranes.

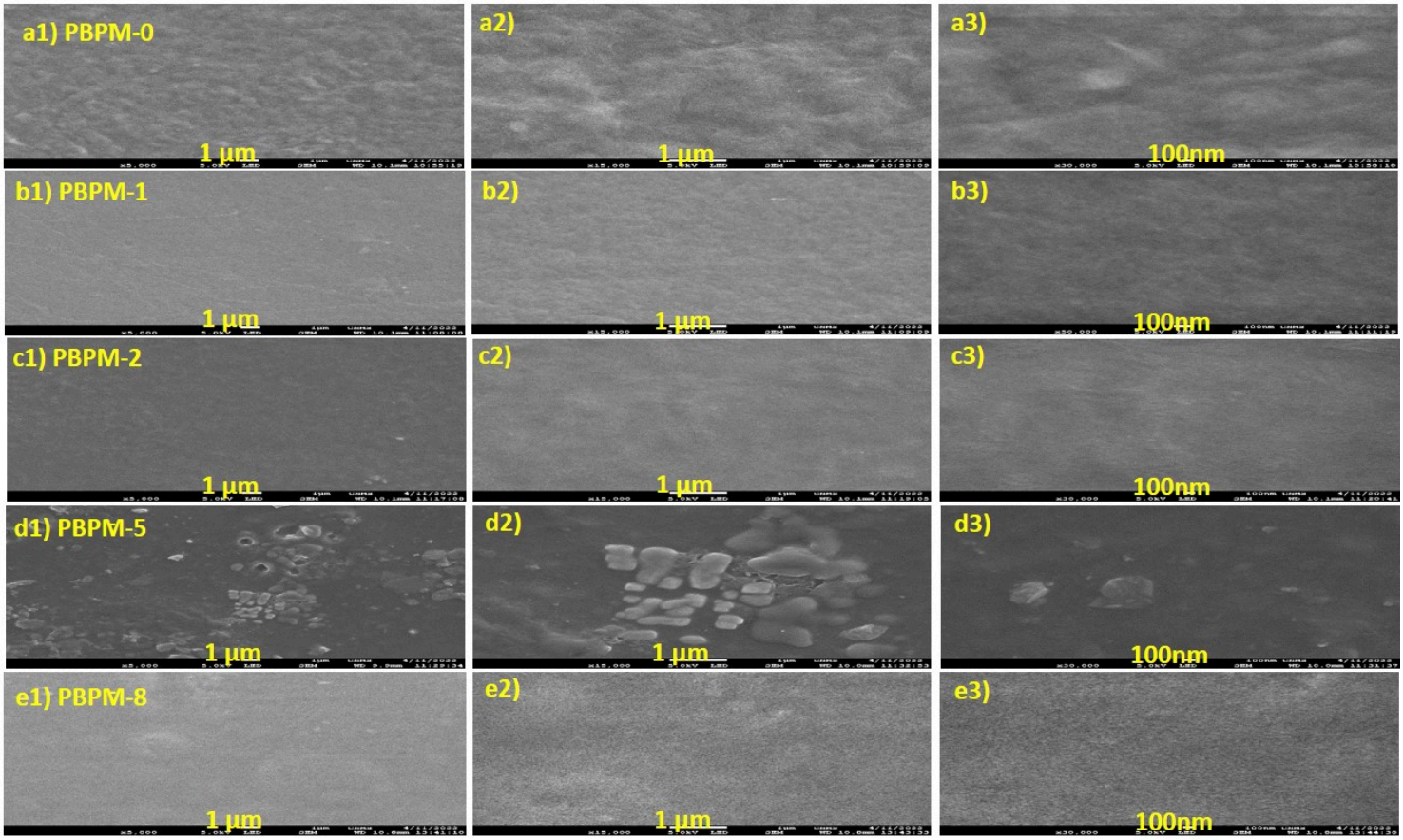


Figure 7

SEM images of pure PEBA and PEBA-PEMA blend membranes.

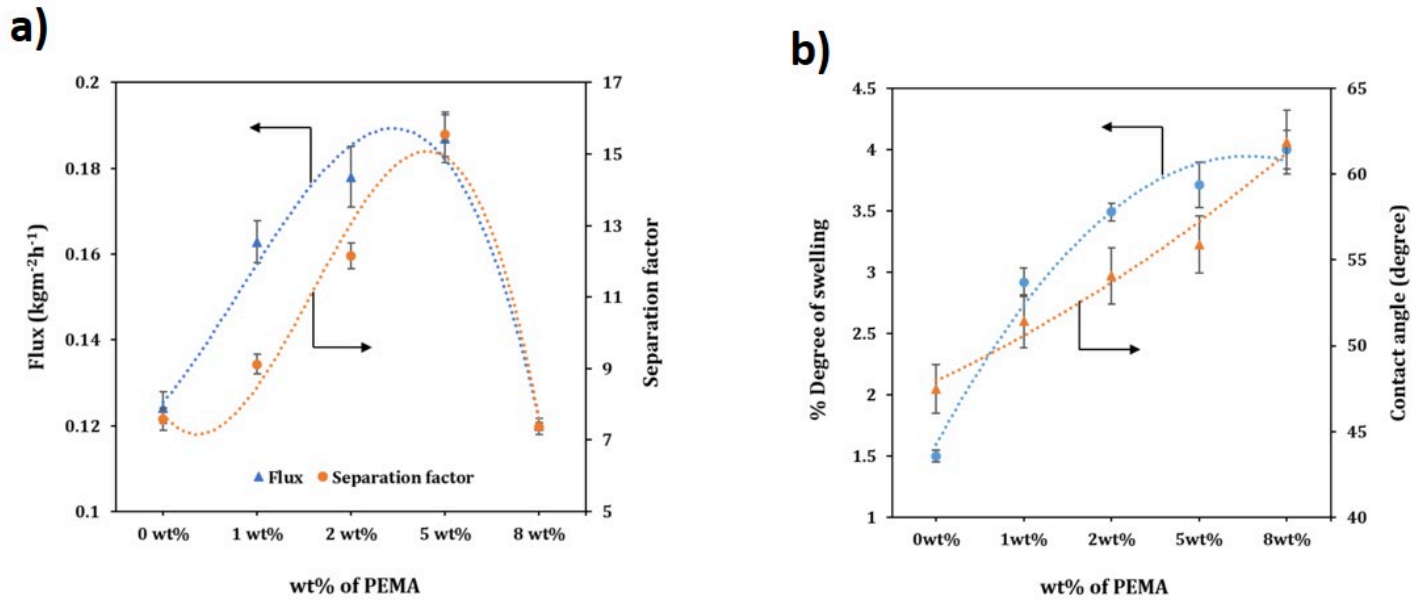


Figure 8

Effect of wt% of PEMA on (a) flux and separation factor; (b) on contact angle measurement and degree of swelling.

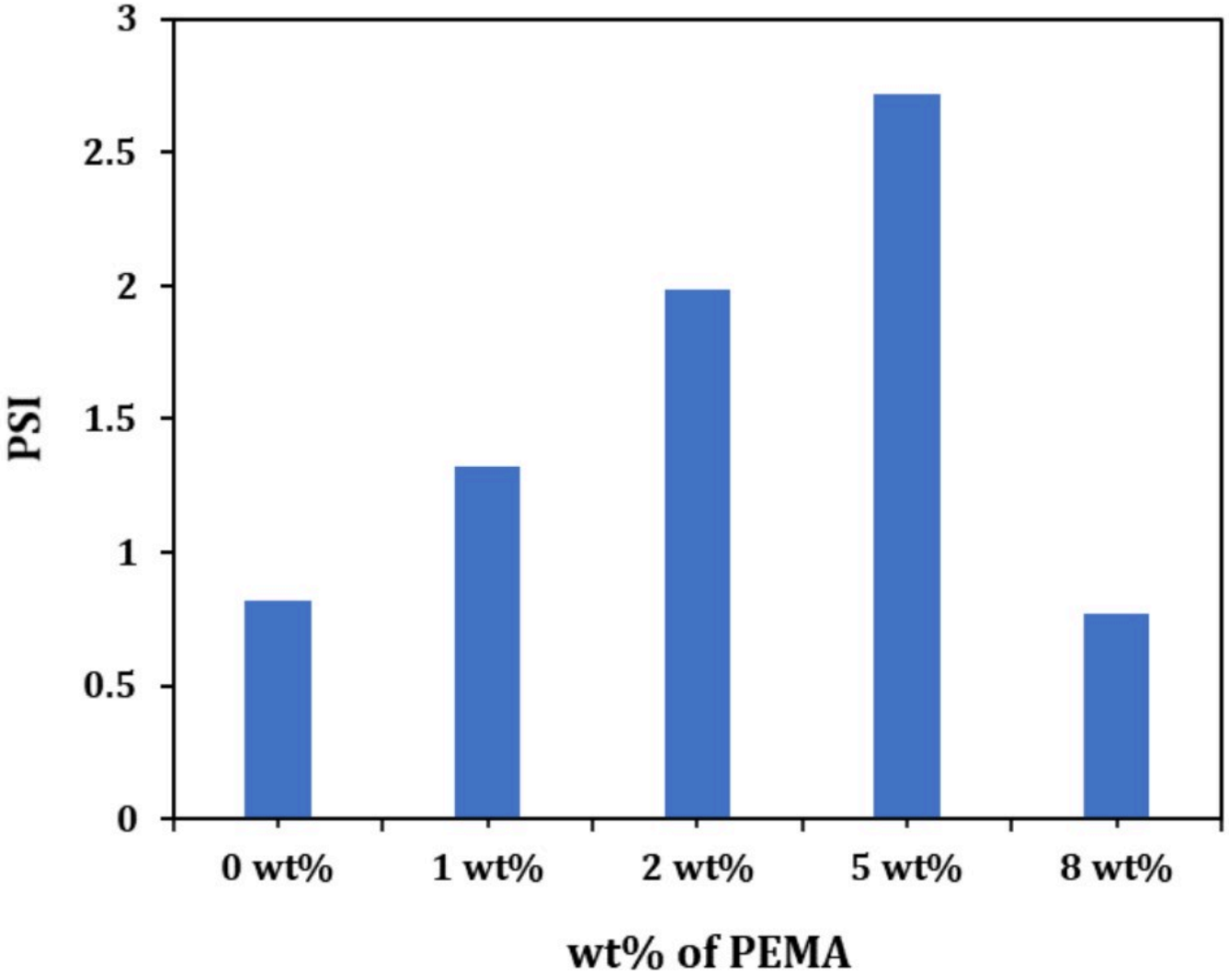


Figure 9

Effect of PEMA wt% on PSI.

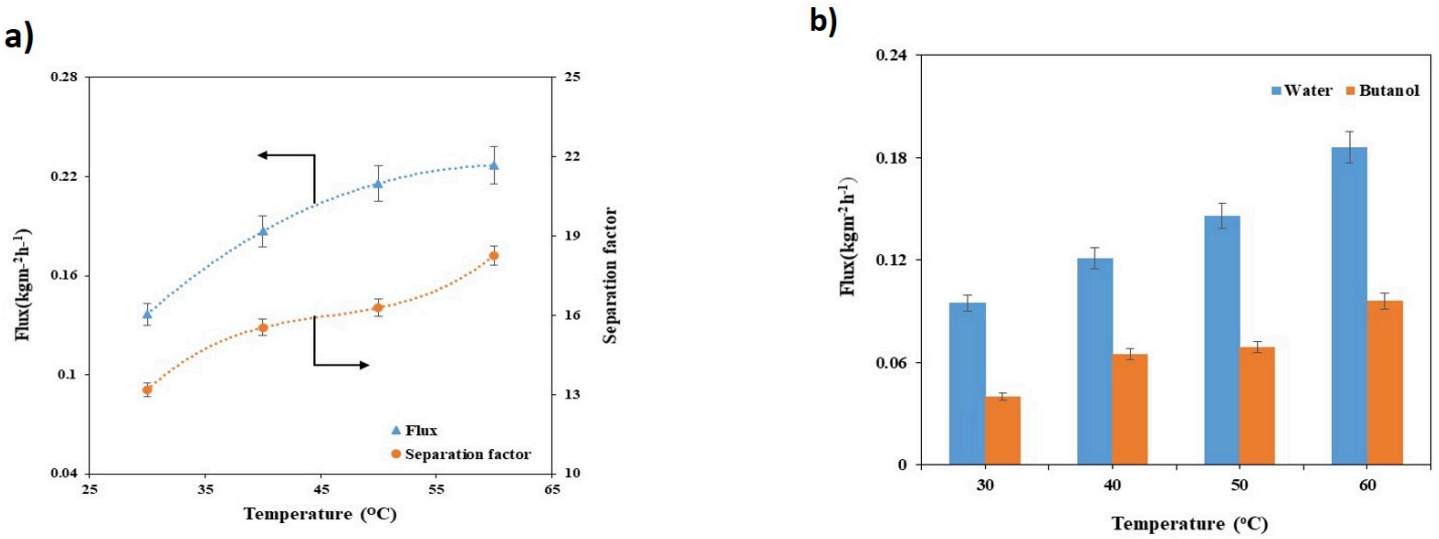


Figure 10

Effect of temperature on (a) total flux and separation factor, (b) water and butanol fluxes.

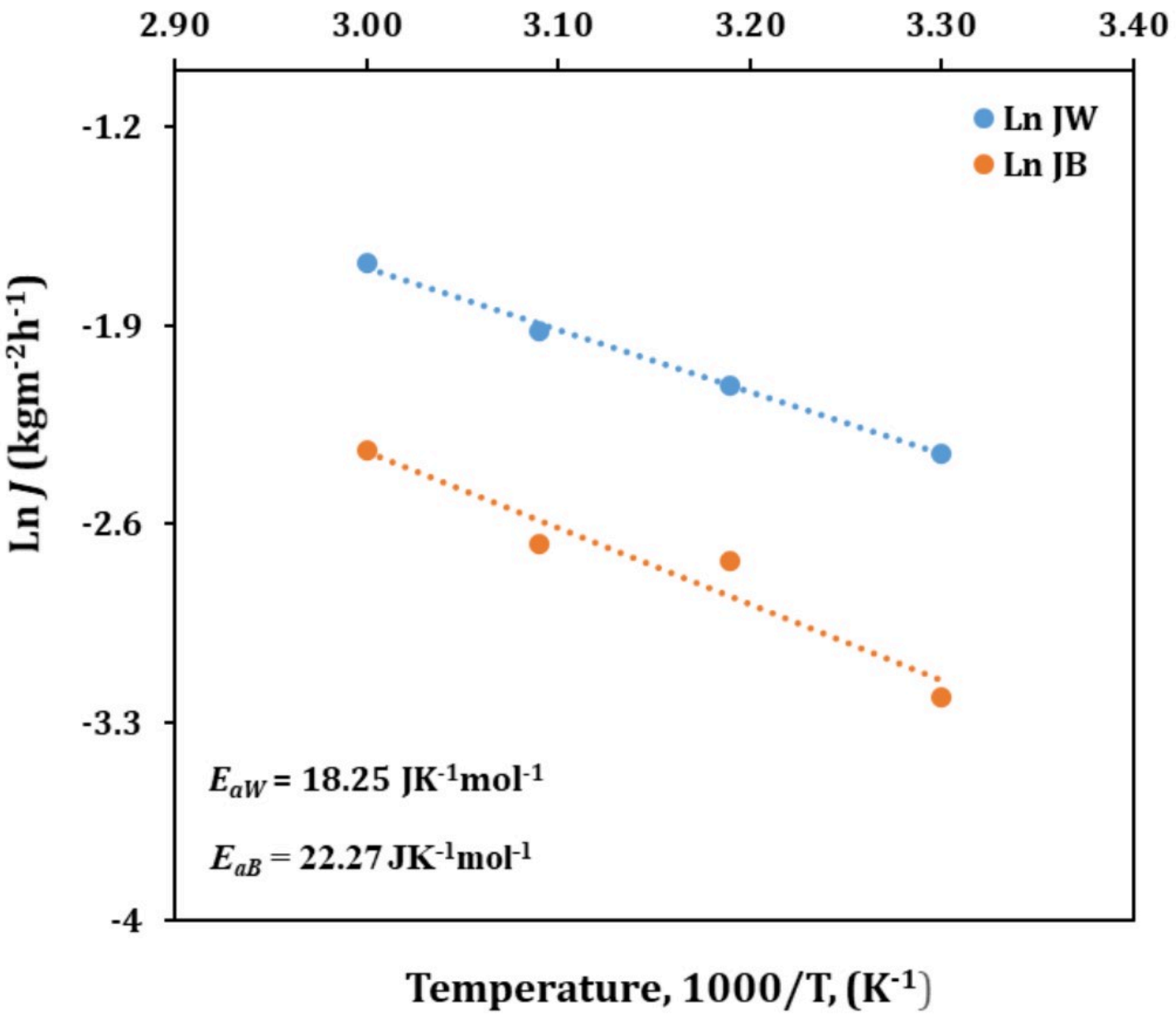


Figure 11

Variation of $\mathrm{Ln}J_W$ and $\mathrm{Ln}J_B$ with temperature.

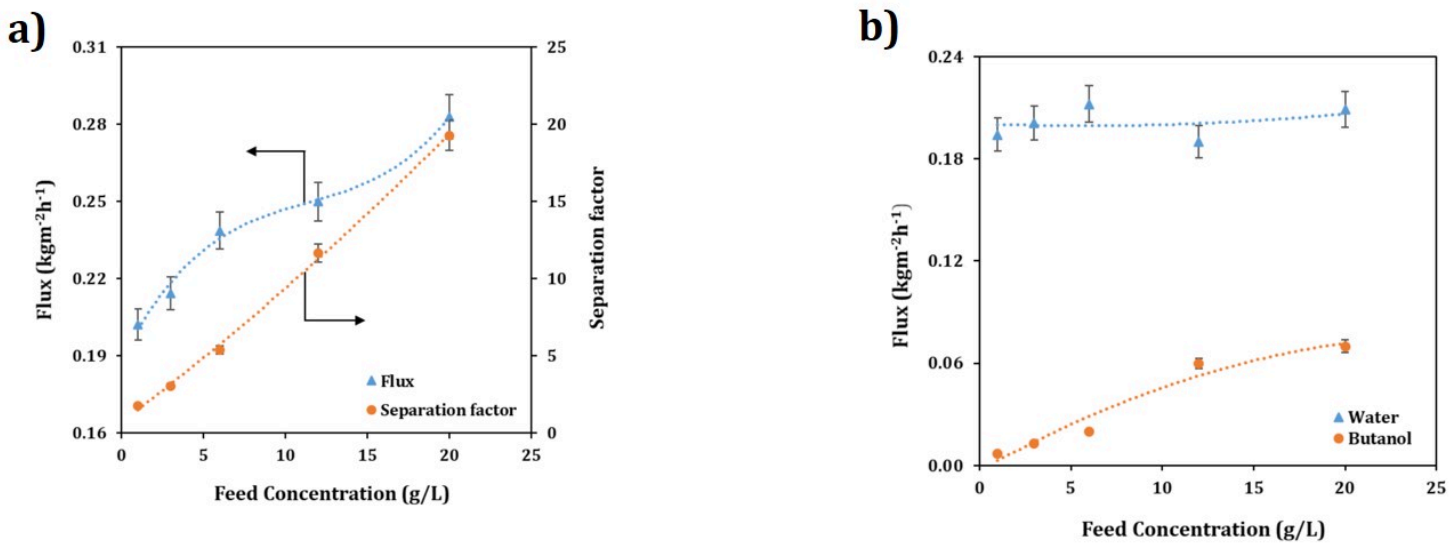


Figure 12

Effect of butanol feed concentration on (a) total flux and separation factor, and (b) butanol and water flux.